

1 Characterisation of Antibody Interactions with the G Protein of Vesicular Stomatitis
2 Virus Indiana Strain and Other Vesiculovirus G Proteins

3 Altar M Munis^{a,b}, Maha Tijani^{a,b}, Mark Hassall^c, Giada Mattiuzzo^c, Mary K Collins^{a,b,d}
4 and Yasuhiro Takeuchi^{a,b}#.

5

6 ^aDivision of Advanced Therapies, National Institute for Biological Standards and
7 Control, South Mimms, UK

8 ^bDivision of Infection and Immunity, University College London, London, UK

9 ^cDivision of Virology, National Institute for Biological Standards and Control, South
10 Mimms, UK

11 ^dOkinawa Institute of Science and Technology, Okinawa, Japan

12

13 Running Title: Interactions between antibodies and vesiculoviruses

14

15 #Correspondence should be addressed to Y.T.

16 Division of Infection and Immunity

17 UCL, Cruciform Building, Room 1.3.11

18 Gower Street

19 London

20 WC1E 6BT

21 United Kingdom

22 Tel: +44 20 3108 2144 (ext 52144).

23 Fax: +44 20 3108 2123

24 (y.takeuchi@ucl.ac.uk)

25

26

27

28

29 **ABSTRACT**

30 Vesicular stomatitis virus Indiana strain G protein (VSVind.G) is the most commonly
31 used envelope glycoprotein to pseudotype lentiviral vectors (LV) for experimental and
32 clinical applications. Recently, G proteins derived from other vesiculoviruses (VesG),
33 for example Cocal virus, have been proposed as alternative LV envelopes with
34 possible advantages compared to VSVind.G. Well-characterised antibodies that
35 recognise VesG will be useful for vesiculovirus research, development of G protein-
36 containing advanced therapy medicinal products (ATMPs), and deployment of
37 VSVind-based vaccine vectors. Here we show that one commercially available
38 monoclonal antibody, 8G5F11, binds to and neutralises G proteins from three strains
39 of VSV as well as Cocal, and Maraba viruses, whereas the other commercially
40 available monoclonal anti-VSVind.G antibody, IE9F9, binds to and neutralises only
41 VSVind.G. Using a combination of G protein chimeras and site-directed mutations,
42 we mapped the binding epitopes of IE9F9 and 8G5F11 on VSVind.G. IE9F9 binds
43 close to the receptor binding site and competes with soluble low-density lipoprotein
44 receptor (LDLR) for binding to VSVind.G, explaining its mechanism of neutralisation.
45 In contrast, 8G5F11 binds close to a region known to undergo conformational changes
46 when the G protein moves to its post-fusion structure, and we propose that 8G5F11
47 cross-neutralises VesGs by inhibiting this.

48 **IMPORTANCE**

49 VSVind.G is currently regarded as the gold-standard envelope to pseudotype lentiviral
50 vectors. However, recently other G proteins derived from vesiculoviruses have been
51 proposed as alternative envelopes. Here, we investigated two anti-VSVind.G
52 monoclonal antibodies for their ability to cross-react with other vesiculovirus G
53 proteins, and identified the epitopes they recognise, and explored the mechanisms
54 behind their neutralisation activity. Understanding how cross-neutralising antibodies
55 interact with other G proteins may be of interest in the context of host-pathogen
56 interaction and co-evolution as well as providing the opportunity to modify the G
57 proteins and improve G protein-containing medicinal products and vaccine vectors.

58

59 **INTRODUCTION**

60 The rhabdovirus, vesicular stomatitis virus Indiana stain (VSVind), has been used
61 ubiquitously as a model system to study humoral and cellular immune responses in
62 addition to being a promising virus for oncolytic virotherapy against cancer (1-3).
63 Furthermore, its single envelope G protein (VSVind.G) is the most commonly used
64 envelope to pseudotype lentiviral vectors and serves as the gold-standard in many
65 experimental and clinical studies (4-6). Both receptor recognition and membrane
66 fusion of the wild-type virus, as well as the pseudotyped particles, are mediated by this
67 single transmembrane viral glycoprotein that homotrimerises and protrudes from the
68 viral surface (7-9). Recently G proteins derived from other vesiculovirus subfamily
69 members, namely, Cocal, Piry, and Chandipura viruses, have been proposed as
70 alternative envelopes for lentiviral vector production due to some possible advantages
71 over VSVind.G (10-12).

72 Although some antigenic and biochemical characteristics of VSVind.G have been
73 reported (1, 7, 13-20), there is still little known about the other vesiculovirus G proteins
74 (VesG) and there is a general lack of reagents commercially available to identify,
75 detect, and characterise them. In the past, monoclonal antibodies (mAbs) have been
76 used to extensively study the antigenic determinants found on viral glycoproteins, e.g.
77 hemagglutinin (HA) of influenza virus, the gp70 protein of murine leukaemia virus
78 (MLV), and rabies virus G protein (21-25). These previous studies, especially on the
79 influenza virus strains and the rabies virus have led to invaluable findings on the
80 structure and function of the glycoproteins allowing identification of epitopes essential
81 in virus neutralisation (25-27). In addition, mAbs have proven useful in viral
82 pathogenesis studies as mutants selected by antibodies, in many cases demonstrated
83 altered pathogenicity to their wild-type counterparts (28-30). Therefore, identification
84 of antibodies that recognise VesG will not only be extremely valuable for vesiculovirus
85 research but also aid in the development of G protein-containing advanced therapy
86 medicinal products (ATMP) and vaccine vectors.

87 Here we show two anti-VSVind.G antibodies, 8G5F11 and a goat polyclonal antibody,
88 VSV-Poly (31, 32), can cross-react with a variety of the VesG and cross-neutralise
89 VesG-LV. We also demonstrate that the other commercially available extracellular
90 monoclonal anti-VSVind.G antibody IE9F9 lacks this cross-reactivity. We further

91 characterise the two mAbs, 8G5F11 and IE9F9, with regards to their relative affinities
92 towards various VesG, binding epitopes, and cross-neutralisation strengths.

93

94 **RESULTS**

95 **Investigation of antibody cross-reactivity with VesG**

96 To investigate antibody binding to different vesiculovirus envelope glycoproteins (G
97 proteins), we prepared plasmid pMD2-based vectors expressing six different
98 vesiculovirus G proteins (VesG): VSVind.G, Cocal virus G (COCV.G), Vesicular
99 stomatitis virus New Jersey strain G (VSVnj.G), Piry virus G (PIRYV.G), Vesicular
100 stomatitis virus Alagoas strain G (VSVala.G), and Maraba virus G (MARAV.G) (Figure
101 1A). HEK293T cells were transfected with these plasmid constructs, stained with the
102 different antibodies, and analysed via flow cytometry. While IE9F9 only bound to
103 VSVind.G, anti-VSVind.G monoclonal antibody 8G5F11 and VSV-Poly both could
104 recognise various VesG with varying binding strengths (Figure 1B). PIRYV.G, the
105 most distant vesiculovirus G investigated with approximately 40% identity to VSVind.G
106 on amino acid level, could be recognised by VSV-Poly while 8G5F11 did not bind to
107 it.

108 **Characterisation of IE9F9 binding, 8G5F11 cross-reactivity and its affinity** 109 **towards other VesG**

110 To confirm that the difference of 8G5F11 binding to VesG was indicative of the mAb
111 affinity towards VesG and not a difference in relative expression levels of the G
112 proteins, we synthesised chimeric G proteins. The endogenous transmembrane and
113 C-terminal domains of VesG were switched with that of VSVind.G (Figure 2A).
114 Following the expression of these chimeric G proteins in HEK293T cells, we
115 investigated 8G5F11 and IE9F9 binding saturation using quantitative flow cytometry
116 while the relative expression levels of the G proteins were monitored using an
117 intracellular anti-VSVind.G mAb, P5D4 (Figure 2B). 8G5F11 showed a wide range of
118 affinities towards VesG: while its affinity for MARAV.G was comparable to that of
119 VSVind.G, its interactions with COCV.G and VSVnj.G were much weaker.

120 To consolidate this finding, we further investigated these mAb-G protein interactions
121 via surface plasmon resonance. First, to quantify mAb binding to G protein monomers
122 under conformationally correct folding, we immobilised wild-type (wt) VSVind.G
123 produced by thermolysin limited proteolysis of viral particles (Gth) (7, 17) and tested
124 the dose-dependent binding of the two mAbs (Figure 2C-D). The measured Kd values

125 for 8G5F11 and IE9F9 binding to VSVind.G were 2.76nM and 14.7nM respectively.
126 To further analyse the VesG-8G5F11 interaction we immobilised the mAb and
127 investigated VesG pseudotyped lentiviral vector (LV) binding. Since pseudotyped LV
128 particles contain many trimeric G protein spikes (33), the analysis of the interaction
129 between VesG binding to immobilised 8G5F11 reflects avidity. Dose-response
130 binding of VSVind.G resulted in a strong response implying high avidity.
131 (Supplementary Figure S1). When identical doses of VesG-LV at 1×10^8 TU/ml were
132 injected on immobilized 8G5F11, similar patterns of binding were observed to that of
133 quantitative flow cytometry, in the order of strength of VSVind > MARAV > VSVala >
134 Cocal > VSVnj (Figure 2E). Unrelated RDpro envelope pseudotyped LVs were utilised
135 as negative control to deduce unspecific interaction of enveloped particles with
136 immobilised mAb. PIRYV.G-LV demonstrated a similar response to that of RDpro-LV
137 indicative of the lack of binding between the G protein and 8G5F11.

138 **Determining the cross-neutralisation abilities of anti-VSVind.G antibodies**

139 These three antibodies were evaluated for their ability to neutralise VSVind.G and
140 VesG pseudotyped LVs (Figure 3). 8G5F11 demonstrated varying strengths of
141 neutralisation against VesG pseudotyped LVs, IC50 values ranging from 11.5ng/ml to
142 86.9 μ g/ml (Figure 3A). There was however limited correlation between G proteins'
143 binding strength and sensitivity of LV, e.g. VSVnj.G-LV was more sensitive than
144 COCV.G-LV (Figure 3A) while COCV.G binding was stronger (Figure 1 and 2). IE9F9
145 neutralised only VSVind.G-LV at 137ng/ml IC50, about 12-fold weaker than 8G5F11
146 (Figure 3B). In the case of VSV-Poly, we only observed cross neutralisation at high
147 serum concentrations (Figure 3C). Furthermore, although VSV-Poly bound to
148 PIRYV.G, it did not neutralise PIRYV.G-LVs.

149 **Mapping the epitopes of anti-VSVind.G mAbs and identification of key amino** 150 **acid residues that dictate antibody binding and neutralisation**

151 To map where the neutralising antibodies might bind to on the G protein surface a
152 series of chimeric G proteins between VSVind.G and COCV.G were constructed. The
153 initial binding and neutralisation studies performed with these chimeras enabled us to
154 narrow down the epitopes of these mAbs to lie between amino acid (aa) residues 137-

155 369¹ on VSVind.G (Supplementary Figure S2). Furthermore, looking at previously
156 published data on 8G5F11 and IE9F9's epitopes obtained through mutant virus
157 escape assays (1, 13-15) we concentrated on two distinct regions on VSVind.G and
158 synthesized 22 different mutant G proteins to study the epitopes (Figure 4). The
159 mutants were cloned into the pMD2 backbone and their functionality were investigated
160 via LV infection and antibody binding assays. All G proteins were confirmed to be
161 functional and could successfully pseudotype LVs yielding comparable titres to their
162 wild-type (wt) counterparts. Furthermore, their relative expression levels were
163 monitored by intracellular P5D4 which also recognises the intracellular domain of
164 COCV.G. Lastly, they could be detected by extracellular VSV-Poly implying there
165 weren't any substantial protein display issues (Supplementary Figure S3).

166 We first investigated antibody binding to these G proteins via flow cytometry. Relative
167 expression levels of the mutants were determined by extracellular VSV-Poly and
168 intracellular P5D4 stains. For both sets the relative difference between expression
169 levels of mutant and wt proteins was in most cases less than two-fold (Figure 5A-B).
170 In the case of 8G5F11, binding to VSVind.G mutants was reduced by approximately
171 100-fold while the changes on COCV.G enabled these mutants to bind to 8G5F11 at
172 similar levels to that of wt VSVind.G (Figure 5C). This change in binding could also
173 be observed on a western blot. While none of the VSVind.G mutants could be
174 visualized, 8G5F11 could bind to COCV.G chimera C8.3 (data not shown). It can be
175 inferred from these results that aa 257-259 (DKD) are the main residues that dictate
176 8G5F11 binding to G proteins.

177 On the other hand, for IE9F9 no statistically significant changes in antibody binding
178 were observed for VSVind.G mutants (data not shown) except for chimeras V1.2 and
179 V1.4 (Figure 5D). However, there was a substantial gain of binding effect for COCV.G
180 mutants. While IE9F9 doesn't bind to wt COCV.G, mutations of amino acid residues
181 LSR and AA (Figure 4) alone led to significant increase in the fluorescence signal, thus
182 antibody binding, C1.4 with both LSR and AA had a comparable MFI level to that of
183 wt VSVind.G.

¹ It should be noted that the amino acid sequence of the full-length G proteins (including the signal peptide) were referred to in this manuscript. Accordingly, reference to specific residue numbers is made in the context of these full-length sequences.

184 Neutralisation profile of both VSVind.G and COCV.G mutants was also examined
185 (Figure 5E-H). While LVs pseudotyped with VSVind.G mutants were not neutralised
186 (Figure 5E), varying degrees of sensitivity were observed for COCV.G mutants with
187 the strongest binder being the most sensitive (Figure 5F). On the other hand, this was
188 not the case for IE9F9 mutants. While dose-dependent neutralisation of V1.2-LV was
189 observed, VSVind.G mutant V1.4-LV was resistant to IE9F9 neutralisation (Figure
190 5G). Furthermore, no effect was observed on COCV.G mutant LV infection even
191 though all bound to the mAb, some at similar levels to wt VSVind.G (Figure 5H). The
192 data shows that while 8G5F11 employs a neutralisation mechanism that is universally
193 effective amongst the tested VesG, IE9F9's is VSVind.G specific and binding does not
194 necessarily result in neutralisation.

195 **Investigation of neutralisation mechanisms utilised by the mAbs: binding**
196 **competition with low-density lipoprotein receptor (LDLR)**

197 Antibodies neutralise viruses and viral vectors by several mechanisms. Many
198 neutralising antibodies (NAbs) prevent virions from interacting with cellular receptors
199 (34). VSVind.G's major receptor has been identified as the low-density lipoprotein
200 receptor (LDLR) (33, 35). Therefore, we investigated the binding competition between
201 8G5F11 and IE9F9 with LDLR via SPR as a potential neutralisation mechanism for
202 the mAbs (Figure 6). Gth immobilised on the chip surface was saturated with repeated
203 injections of 8G5F11 and IE9F9. This was followed by an injection of recombinant
204 soluble human LDLR (sLDLR) and its binding to Gth was examined. While sLDLR
205 was able to bind to Gth following 8G5F11 saturation as well as Gth without antibody
206 exposure (buffer control), this interaction was almost completely abrogated by IE9F9.
207 These data suggest that IE9F9, but not 8G5F11, neutralises VSVind.G-LV by blocking
208 the G protein-receptor interaction either through steric hindrance or direct competition.

209 **DISCUSSION**

210 VSVind.G is the most commonly used envelope glycoprotein to pseudotype LVs for
211 experimental and clinical applications. VSVind.G pseudotyped LVs can be produced
212 in high titres and can infect a range of target cells. However, VSVind.G is cytotoxic to
213 cells; thus, it is difficult to express it constitutively (36, 37). Moreover, VSVind.G
214 pseudotyped LVs can be inactivated by human serum complement which limits their
215 potential *in vivo* use (38-42). Therefore, there is a clear need for alternative envelopes

216 to pseudotype LVs. Some of the most recent alternative envelopes that have been
217 utilised are the G proteins of the other vesiculovirus family members (10-12).
218 However, one drawback of using these new G proteins is that there are no reagents
219 commercially available to identify or characterise them.

220 In this report, we have demonstrated that 8G5F11 monoclonal antibody can, unlike
221 VSVind.G specific IE9F9, cross-react with a variety of the VesG and cross-neutralise
222 VesG-LV. Furthermore, we characterised a goat anti-VSVind.G polyclonal antibody
223 which also can bind and neutralise a wide range of vesiculovirus G proteins.

224 The cross-reactive monoclonal 8G5F11 demonstrated interesting characteristics. Its
225 high cross-reactivity even towards more distant relatives of VSVind.G such as
226 VSVnj.G suggested that it might be recognising a well-conserved epitope. However,
227 the results of the binding saturation assay didn't correlate with phylogenetic relativity.
228 It revealed that its affinity towards COCV.G, one of the closest relatives of VSVind.G,
229 was one of the weakest amongst the VesG investigated with almost a 250-fold
230 difference compared to VSVind.G (Figure 2B).

231 This discrepancy can be explained through fine mapping of the 8G5F11 epitope. We
232 identified the amino acids 257-259, DKD, as the key residues on VSVind.G for 8G5F11
233 binding. On VSVind.G the two negatively charged aspartic acid residues flank the
234 positively charged lysine possibly contributing towards the structure of the α -helix form
235 through salt-bridges (7, 16, 17). When either of the aspartic acid residues is mutated
236 to a neutral residue a significant reduction in binding is observed. When this is
237 compared to the corresponding three residues on other VesG, the antibody binding is
238 dependent on the overall charge of these three residues rather than the ones
239 surrounding them. In MARAV.G, these residues are identical to VSVind.G, explaining
240 why the antibody has similar strength of binding to these two G proteins
241 (Supplementary Figure S4). On the other hand, VSVala.G binds 8G5F11 with high
242 affinity although these residues are not fully conserved, as in VSVala.G the second
243 aspartic acid residue is replaced with a glutamic acid. But it is possible that the
244 conservation of the second negative charge and the structural similarities between
245 these two residues enable a robust G protein-antibody interaction. Lastly, VEQ
246 corresponding aa residues in PIRYV.G, VEQ, have electrostatically and structurally

247 different characteristics to that of lysine and aspartic acid leading to the lack of
248 interaction between the mAb and G protein.

249 We showed that IE9F9 recognises a β -sheet rich domain of the G protein (7, 17). A
250 complete abrogation of binding wasn't observed with the VSVind.G mutants produced.
251 This implies that the antibody either relies on other structural cues and environmental
252 charges around for binding or can utilise a secondary epitope. However, through the
253 gain of binding effect observed in COCV.G mutants, we were able to identify two
254 regions; AA and LSR, aa residues 352-353 and 356-358 respectively on VSVind.G,
255 that are the key to this antibody's interaction.

256 All three reagents investigated demonstrated neutralising activities. 8G5F11 had the
257 greatest ability to cross-neutralise a wide array of vesiculovirus family members. The
258 strength of neutralisation for this mAb, however, didn't correlate with its affinity towards
259 other VesG (Figure 2 and 3). This suggests that innate differences, such as protein
260 structure, between the VesG might be playing a role in LV neutralisation. Since the
261 structures of the VesG other than VSVind.G and CHAV.G are not yet delineated, it is
262 hard to accurately point out the key factors and mechanism involved. However, we
263 have identified 8G5F11's epitope to lie close to the cross-over point between pleckstrin
264 homology and trimerisation domain of VSVind.G (7, 17, 19, 20, 35). Several hinge
265 segments have been identified in the proximity of the epitope which undergo large
266 rearrangements in its relative orientation while the G protein refolds from pre to post-
267 fusion conformation in the low-pH conditions of the endosomes following endocytosis
268 (16, 19, 35). It can be hypothesised that 8G5F11 might be hindering this process
269 ultimately preventing viral fusion and infection. As pH-induced conformational
270 changes during viral fusion is a shared characteristic amongst VesG (43), this might
271 be the underlying reason behind 8G5F11's ability to cross-neutralise VesG-LV.

272 We have shown that IE9F9 blocks VSVind.G binding to its major receptor LDLR
273 (Figure 6). The crystal structures of VSVind.G in complex with LDLR domains have
274 been recently identified and have shown that VSVind.G can interact with two distinct
275 cysteine-rich domains (CR2 and CR3) of LDLR (35). One of the regions on VSVind.G
276 that is crucial for LDLR CR domain binding lies between amino acids 366-370, only
277 seven amino acids away from the key residues in IE9F9's epitope. The key residues
278 in this region of VSVind.G are not conserved amongst vesiculoviruses therefore,

279 neither the use of this epitope nor LDLR can be generalised to the other members of
280 the genus, making IE9F9's epitope and neutralisation mechanism specific to
281 VSVind.G. The lack of cross-reactivity and cross-neutralisation (Figure 1 and 3)
282 displayed by the mAb towards VesG as well as its failure to neutralise COCV.G
283 mutants when its epitope is inserted into the G protein (Figure 5) suggest specific
284 requirement for binding mode between IE9G9 and G proteins to result in
285 neutralisation. Nikolic and colleagues have demonstrated that VSVind.G has
286 specifically evolved to interact with the CR domains of other LDLR family members
287 (35). The other members of the receptor family have already been identified as
288 secondary ports of entry for the virus (33). Complete neutralisation achieved with
289 IE9F9 indicates that the other LDLR family members might be interacting with the
290 same epitope on VSVind.G as well.

291 Further work on these two identified epitopes regarding their immunodominance in an
292 *in vivo* setting and their detailed characterisation on other VesG from the structure-
293 function point of view may be of interest in the context of host-pathogen interaction
294 and co-evolution. This may also provide the opportunity for modifying VSVind.G to
295 improve G protein-containing advanced therapy medicinal products and VSVind-
296 based vaccine vectors.

297

298 REFERENCES

- 299 1. Keil W, Wagner RR. 1989. Epitope mapping by deletion mutants and chimeras of two
300 vesicular stomatitis virus glycoprotein genes expressed by a vaccinia virus vector. *Virology*
301 170:392-407.
- 302 2. Wagner RR. 1987. Rhabdovirus biology and infection: An overview., p 9-74. *In* Wagner RR
303 (ed), *The Rhabdoviruses*. Plenum, New York.
- 304 3. Hastie E, Grdzlishvili VZ. 2012. Vesicular stomatitis virus as a flexible platform for oncolytic
305 virotherapy against cancer. *Journal of General Virology* 93:2529-2545.
- 306 4. Naldini L, Blomer U, Gallay P, Ory D, Mulligan R, Gage FH, Verma IM, Trono D. 1996. In vivo
307 gene delivery and stable transduction of nondividing cells by a lentiviral vector. *Science*
308 272:263-267.
- 309 5. Bhella RS, Nichol ST, Wanas E, Ghosh HP. 1998. Structure, expression and phylogenetic
310 analysis of the glycoprotein gene of Cocal virus. *Virus Res* 54:197-205.
- 311 6. Reiser J, Harmison G, KluepfelStahl S, Brady RO, Karlson S, Schubert M. 1996. Transduction
312 of nondividing cells using pseudotyped defective high-titer HIV type 1 particles. *Proceedings*
313 *of the National Academy of Sciences of the United States of America* 93:15266-15271.
- 314 7. Roche S, Rey FA, Gaudin Y, Brassanelli S. 2007. Structure of the pre-fusion form of the
315 vesicular stomatitis virus
316 glycoprotein g. *Science* 315:843-848.
- 317 8. Bishop DH, Repik P, Obijeski JF, Moore NF, Wagner RR. 1975. Restitution of infectivity to
318 spikeless vesicular stomatitis virus by solubilized viral components. *J Virol* 16:75-84.
- 319 9. Matlin KS, Reggio H, Helenius A, Simons K. 1982. Pathway of vesicular stomatitis virus entry
320 leading to infection. *J Mol Biol* 156:609-31.
- 321 10. Humbert O, Gisch DW, Wohlfahrt ME, Adams AB, Greenberg PD, Schmitt TM, Trobridge GD,
322 Kiem HP. 2016. Development of Third-generation Cocal Envelope Producer Cell Lines for
323 Robust Lentiviral Gene Transfer into Hematopoietic Stem Cells and T-cells. *Mol Ther*
324 24:1237-46.
- 325 11. Trobridge GD, Wu RA, Hansen M, Ironside C, Watts KL, Olsen P, Beard BC, Kiem HP. 2010.
326 Cocal-pseudotyped lentiviral vectors resist inactivation by human serum and efficiently
327 transduce primate hematopoietic repopulating cells. *Mol Ther* 18:725-33.
- 328 12. Hu S, Mohan Kumar D, Sax C, Schuler C, Akkina R. 2016. Pseudotyping of lentiviral vector
329 with novel vesiculovirus envelope glycoproteins derived from Chandipura and Piry viruses.
330 *Virology* 488:162-8.
- 331 13. Lefrancois L, Lyles DS. 1983. Antigenic determinants of vesicular stomatitis virus: analysis
332 with antigenic variants. *J Immunol* 130:394-8.
- 333 14. Lefrancois L, Lyles DS. 1982. The interaction of antibody with the major surface glycoprotein
334 of vesicular stomatitis virus. I. Analysis of neutralizing epitopes with monoclonal antibodies.
335 *Virology* 121:157-67.
- 336 15. Vandepol SB, Lefrancois L, Holland JJ. 1986. Sequences of the major antibody binding
337 epitopes of the Indiana serotype of vesicular stomatitis virus. *Virology* 148:312-25.
- 338 16. Roche S, Albertini AAV, Lepault J, Bressanelli S, Gaudin Y. 2008. Structures of vesicular
339 stomatitis virus glycoprotein: membrane fusion revisited. *Cellular and Molecular Life*
340 *Sciences* 65:1716-1728.
- 341 17. Roche S, Bressanelli S, Rey FA, Gaudin Y. 2006. Crystal structure of the low-pH form of the
342 vesicular stomatitis virus glycoprotein G. *Science* 313:187-91.
- 343 18. Albertini AA, Merigoux C, Libersou S, Madiona K, Bressanelli S, Roche S, Lepault J, Melki R,
344 Vachette P, Gaudin Y. 2012. Characterization of Monomeric Intermediates during VSV
345 Glycoprotein Structural Transition. *Plos Pathogens* 8.

- 346 19. Baquero E, Albertini AA, Raux H, Abou-Hamdan A, Boeri-Erba E, Ouldali M, Buonocore L,
347 Rose JK, Lepault J, Bressanelli S, Gaudin Y. 2017. Structural intermediates in the fusion-
348 associated transition of vesiculovirus glycoprotein. *EMBO J* 36:679-692.
- 349 20. Baquero E, Albertini AA, Vachette P, Lepault J, Bressanelli S, Gaudin Y. 2013. Intermediate
350 conformations during viral fusion glycoprotein structural transition. *Current Opinion in*
351 *Virology* 3:143-150.
- 352 21. Benmansour A, Leblois H, Coulon P, Tuffereau C, Gaudin Y, Flamand A, Lafay F. 1991.
353 Antigenicity of Rabies Virus Glycoprotein. *Journal of Virology* 65:4198-4203.
- 354 22. Lubeck MD, Gerhard W. 1981. Topological mapping antigenic sites on the influenza
355 A/PR/8/34 virus hemagglutinin using monoclonal antibodies. *Virology* 113:64-72.
- 356 23. Webster RG, Laver WG. 1980. Determination of the number of nonoverlapping antigenic
357 areas on Hong Kong (H3N2) influenza virus hemagglutinin with monoclonal antibodies and
358 the selection of variants with potential epidemiological significance. *Virology* 104:139-48.
- 359 24. Stone MR, Nowinski RC. 1980. Topological mapping of murine leukemia virus proteins by
360 competition-binding assays with monoclonal antibodies. *Virology* 100:370-81.
- 361 25. Seif I, Coulon P, Rollin PE, Flamand A. 1985. Rabies virulence: effect on pathogenicity and
362 sequence characterization of rabies virus mutations affecting antigenic site III of the
363 glycoprotein. *J Virol* 53:926-34.
- 364 26. Wiley DC, Wilson IA, Skehel JJ. 1981. Structural identification of the antibody-binding sites of
365 Hong Kong influenza haemagglutinin and their involvement in antigenic variation. *Nature*
366 289:373-8.
- 367 27. Hovanec DL, Air GM. 1984. Antigenic structure of the hemagglutinin of influenza virus
368 B/Hong Kong/8/73 as determined from gene sequence analysis of variants selected with
369 monoclonal antibodies. *Virology* 139:384-92.
- 370 28. Dietzschold B, Wunner WH, Wiktor TJ, Lopes AD, Lafon M, Smith CL, Koprowski H. 1983.
371 Characterization of an antigenic determinant of the glycoprotein that correlates with
372 pathogenicity of rabies virus. *Proc Natl Acad Sci U S A* 80:70-4.
- 373 29. Spriggs DR, Fields BN. 1982. Attenuated reovirus type 3 strains generated by selection of
374 haemagglutinin antigenic variants. *Nature* 297:68-70.
- 375 30. Zondag GCM, Postma FR, Van Etten I, Verlaan I, Moolenaar WH. 1998. Sphingosine 1-
376 phosphate signalling through the G-protein-coupled receptor Edg-1. *Biochemical Journal*
377 330:605-609.
- 378 31. Tamura K, Oue A, Tanaka A, Shimizu N, Takagi H, Kato N, Morikawa A, Hoshino H. 2005.
379 Efficient formation of vesicular stomatitis virus pseudotypes bearing the native forms of
380 hepatitis C virus envelope proteins detected after sonication. *Microbes and Infection* 7:29-
381 40.
- 382 32. Hoshino H, Nakamura T, Tanaka Y, Miyoshi I, Yanagihara R. 1993. Functional conservation of
383 the neutralizing domains on the external envelope glycoprotein of cosmopolitan and
384 melanesian strains of human T cell leukemia/lymphoma virus type I. *J Infect Dis* 168:1368-
385 73.
- 386 33. Finkelshtein D, Werman A, Novick D, Barak S, Rubinstein M. 2013. LDL receptor and its
387 family members serve as the cellular receptors for vesicular stomatitis virus. *Proceedings of*
388 *the National Academy of Sciences of the United States of America* 110:7306-7311.
- 389 34. Klasse PJ. 2014. Neutralization of Virus Infectivity by Antibodies: Old Problems in New
390 Perspectives. *Adv Biol* 2014.
- 391 35. Nikolic J, Belot L, Raux H, Legrand P, Gaudin Y, AA. 2018. Structural basis for the
392 recognition of LDL-receptor family members by VSV glycoprotein. *Nat Commun* 9:1029.
- 393 36. Burns JC, Friedmann T, Driever W, Burrascano M, Yee JK. 1993. Vesicular stomatitis virus G
394 glycoprotein pseudotyped retroviral vectors: concentration to very high titer and efficient
395 gene transfer into mammalian and nonmammalian cells. *Proc Natl Acad Sci U S A* 90:8033-7.

- 396 37. Hoffmann M, Wu YJ, Gerber M, Berger-Rentsch M, Heimrich B, Schwemmler M, Zimmer G.
397 2010. Fusion-active glycoprotein G mediates the cytotoxicity of vesicular stomatitis virus M
398 mutants lacking host shut-off activity. *J Gen Virol* 91:2782-93.
- 399 38. Tesfay MZ, Ammayappan A, Federspiel MJ, Barber GN, Stojdl D, Peng KW, Russell SJ. 2014.
400 Vesiculovirus neutralization by natural IgM and complement. *J Virol* 88:6148-57.
- 401 39. Tesfay MZ, Kirk AC, Hadac EM, Griesmann GE, Federspiel MJ, Barber GN, Henry SM, Peng
402 KW, Russell SJ. 2013. PEGylation of Vesicular Stomatitis Virus Extends Virus Persistence in
403 Blood Circulation of Passively Immunized Mice. *Journal of Virology* 87:3752-3759.
- 404 40. Beebe DP, Cooper NR. 1981. Neutralization of Vesicular Stomatitis-Virus (Vsv) by Human-
405 Complement Requires a Natural Igm Antibody Present in Human-Serum. *Journal of*
406 *Immunology* 126:1562-1568.
- 407 41. DePolo NJ, Reed JD, Sheridan PL, Townsend K, Sauter SL, Jolly DJ, Dubensky TW, Jr. 2000.
408 VSV-G pseudotyped lentiviral vector particles produced in human cells are inactivated by
409 human serum. *Mol Ther* 2:218-22.
- 410 42. Croyle MA, Callahan SM, Auricchio A, Schumer G, Linse KD, Wilson JM, Brunner LJ, Kobinger
411 GP. 2004. PEGylation of a vesicular stomatitis virus G pseudotyped lentivirus vector prevents
412 inactivation in serum. *Journal of Virology* 78:912-921.
- 413 43. Baquero E, Albertini AA, Gaudin Y. 2015. Recent mechanistic and structural insights on class
414 III viral fusion glycoproteins. *Curr Opin Struct Biol* 33:52-60.
- 415 44. Kumar S, Stecher G, Tamura K. 2016. MEGA7: Molecular Evolutionary Genetics Analysis
416 Version 7.0 for Bigger Datasets. *Mol Biol Evol* 33:1870-4.
- 417 45. Jones DT, Taylor WR, Thornton JM. 1992. The rapid generation of mutation data matrices
418 from protein sequences. *Comput Appl Biosci* 8:275-82.
- 419 46. Zufferey R, Nagy D, Mandel RJ, Naldini L, Trono D. 1997. Multiply attenuated lentiviral vector
420 achieves efficient gene delivery in vivo. *Nat Biotechnol* 15:871-5.
- 421 47. Knight S, Sanber K, Stephen S, Ferrareso M, Baley R, Escors D, Santilli G, Thrasher A, Collins
422 M, Takeuchi Y. 2014. A clinical-grade constitutive packaging cell line for the production of
423 self-inactivating lentiviral vectors. *Human Gene Therapy* 25:A101-A102.
- 424 48. Sanber KS, Knight SB, Stephen SL, Bailey R, Escors D, Minshull J, Santilli G, Thrasher AJ,
425 Collins MK, Takeuchi Y. 2015. Construction of stable packaging cell lines for clinical lentiviral
426 vector production. *Scientific Reports* 5.

427

428

429 **MATERIALS AND METHODS**

430 **Cell culture.** In all experiments, HEK293T cells were used. The cell line was
431 maintained in Dulbecco's Modified Eagle Medium (DMEM) (Sigma-Aldrich, St Louis,
432 MO) supplemented with 10% heat-inactivated foetal calf serum (Gibco, Carlsbad, CA),
433 2mM L-Glutamine (Gibco), 50 units/ml Penicillin (Gibco), 50µg/ml Streptomycin
434 (Gibco). All cells were kept in cell culture incubators at 37°C and 5% CO₂.

435 **Phylogenetic analysis of vesiculovirus and rabies virus G proteins based on**
436 **amino acid sequences.** G proteins of the major vesiculoviruses (VSVind, UniProt
437 Accession Number: P03522, Cocal virus, #O56677, VSVnj, #P04882, Piry virus,
438 #Q85213, Maraba virus, #F8SPF4, VSVala, # B3FRL4, Chandipura virus, #P13180,
439 Carajas virus, #A0A0D3R1Y6, Isfahan virus, # Q5K2K4) as well as the G protein of
440 the Rabies virus (#Q8JXF6), were included in the analysis. The amino acid sequences
441 were aligned using ClustalOmega online multiple sequence alignment tool (EMBL-
442 EPI). The evolutionary analyses were conducted in MEGA7 (44). The evolutionary
443 history was inferred by using the maximum likelihood method based on the Jones-
444 Taylor-Thornton matrix-based model (45). The tree with the highest likelihood is
445 shown with the bootstrap confidence values (out of 100) indicated at the nodes. The
446 tree is drawn to scale, with branch lengths measured in the number of substitutions
447 per site, depicted in the linear scale.

448 **Plasmids used in experiments.** VSVind.G expression plasmids, pMD2.G, and gag-
449 pol expression plasmid p8.91 (46) were purchased from Plasmid Factory (Germany).
450 GFP expressing self-inactivating vector plasmid used in the production of lentiviral
451 vectors was produced in our lab previously (47, 48). pMD2.Cocal.G, COCV.G,
452 expression plasmid was a kindly provided by Hans-Peter Kiem (Fred Hutchinson
453 Cancer Research Center, Seattle, WA) . All other VesG envelopes were cloned into
454 this backbone using the restriction enzymes PmlI and EcoRI. Amino acid sequences
455 for VSVnj.G, PIRYV.G, MARAV.G, VSVala.G were retrieved from UniProt. Codon-
456 optimised genes were ordered from Genewiz (South Plainfield, NJ). Unrelated feline
457 endogenous virus RD114 derived RDpro envelope (48) was used as a negative control
458 in several assays.

459 **Gene transfer to mammalian cells.** Single plasmid transfection was used to express
460 VesG on HEK293T cell surface. HEK293T cells were seeded on the day prior to

461 transfection at 4×10^6 cell per 10cm plate. These cells were transfected by lipofection
462 using FuGENE6 (Promega, Madison, WI) according to the manufacturer's
463 instructions. The cells were harvested 48h later to be used in various flow cytometry
464 assays.

465 **Overlapping extension PCR to synthesise VesG chimeras.** Phusion High-Fidelity
466 PCR Kit (NEB, Ipswich, MA) was used to perform the PCR reactions. All primers used
467 were obtained from Sigma-Aldrich (Supplementary Table 1). To splice two DNA
468 molecules, special primers were at the joining ends. For each molecule, the first of two
469 PCRs created a linear insert with a 5' overhang complementary to the 3' end of the
470 sequence from the other gene. Following annealing, these extensions allowed the
471 strands of the PCR product to act as a pair of oversized primers and the two
472 sequences were fused. Once both DNA molecules were extended, a second PCR was
473 carried out with only the flanking primers to amplify the newly created double-stranded
474 DNA of the chimeric gene.

475 **Surface plasmon resonance.** Analyses were performed using a BIAcore T100
476 instrument (GE Healthcare). Gth (0.04 mg/mL) and 8G5F11 (0.03 mg/mL) in sodium
477 acetate buffers (10mM, pH 4.5 and 4.0 respectively) were immobilised on a CM5
478 sensor chip using the amine coupling system according to the manufacturer's
479 instructions. To measure mAb affinity to VSVind.G, 8G5F11 (MW 155kDa) and IE9F9
480 (MW 155kDa) were suspended in HBS-EP (0.01M HEPES pH7.4, 0.15M NaCl, 3mM
481 EDTA, 0.005v/v P20) and passed over the immobilised Gth at the indicated
482 concentrations. To measure VesG-LV avidity against 8G5F11, LV preparations were
483 suspended in HBS-EP buffer and passed over the immobilised mAb at indicated titers.
484 The dissociation constants were calculated using BIAevaluation software according to
485 the manufacturer's instructions. For the competitive binding assay, multiple injections
486 of mAbs at 10 μ g/mL concentration was performed followed by injection of soluble
487 recombinant LDLR (R&D Systems, Minneapolis, MN) at an identical concentration.

488 **Use of molecules of equivalent soluble fluorochrome (MESF) system for**
489 **quantitative flow-cytometry analysis.** Quantum Alexa Fluor 647 MESF kit (Bangs
490 Laboratories, Fishers, IN) was utilised for all quantitative fluorescence flow cytometry
491 experiments. This is a microsphere kit that enables the standardisation of
492 fluorescence intensity units. Beads with a pre-determined number of fluorophores are

493 run on the same day and at the same fluorescence settings as stained cell samples to
494 establish a calibration curve that relates the instrument channel values (i.e. median
495 fluorescence intensity (MFI)) to standardised fluorescence intensity (MESF) units.

496 **SDS/PAGE.** Gth was visualised via Ponceau S staining. 15µg of Gth was boiled at
497 95°C for 5 mins in 5X Laemmli buffer (5% Sodium dodecyl sulfate (SDS), 50% glycerol,
498 0.1% bromophenol blue, 250mM Tris-HCl, pH 6.8, and, 5% β-mercaptoethanol) and
499 resolved on 10% SDS-PAGE gel (10% acrylamide-Tris). Sample was then transferred
500 onto a nitrocellulose membrane (GE Healthcare) and visualised.

501 **Extracellular and intracellular antibody binding assay.** HEK293T cells were
502 transfected to express the G proteins. 48 hours later cells were harvested, washed
503 twice with PBS and plated in U-bottom 96-well plates at identical densities. For
504 intracellular antibody binding assays cells were fixed with 1% formaldehyde (Sigma-
505 Aldrich, St Louis, MO) in PBS, permeabilised using 0.05% saponin (Sigma-Aldrich, St
506 Louis MO) in PBS and blocked with 1% bovine serum albumin (BSA, Sigma-Aldrich,
507 St Louis MO) in PBS. Cells were then incubated with serial dilutions of extracellular
508 and intracellular antibodies ranging from 0.1mg/ml to 2x10⁻⁷ mg/ml in 1% BSA
509 (Sigma) in PBS in a total reaction volume of 200µl. After washing twice, each sample
510 was incubated with its respective fluorophore-conjugated secondary antibody
511 (Antibodies used are listed in Supplementary Table 2). Cells were then washed twice
512 and resuspended in PBS. Stained cell samples were analysed via flow cytometry
513 using a FACSCanto II (BD Biosciences, San Jose, CA) and Flowjo software.

514 **Transient LV production and concentration.** Three-plasmid co-transfection into
515 HEK293T cells was used to make pseudotyped LV as described previously (46).
516 Briefly, 4x10⁶ 293T cells were seeded in 10cm plates. 24 hours later, they were
517 transfected using FuGene6 (Promega, Madison, WI) with following plasmids: SIN pHV
518 (GFP expressing vector plasmid (47, 48)), p8.91 (Gag-Pol expression plasmid (46)),
519 and envelope expression plasmids. The medium was changed after 24 hours and then
520 vector containing media (VCM) was collected over 24-hour periods for 2 days.
521 Following collection, VCM was passed through Whatman Puradisc 0.45µm filters
522 (SLS) and concentrated ~100-fold by ultra-centrifugation at 22,000 rpm (87,119xg) for
523 2 hours at 4°C in Beckmann Optima LK-90 ultracentrifuge using the SW-28 swinging

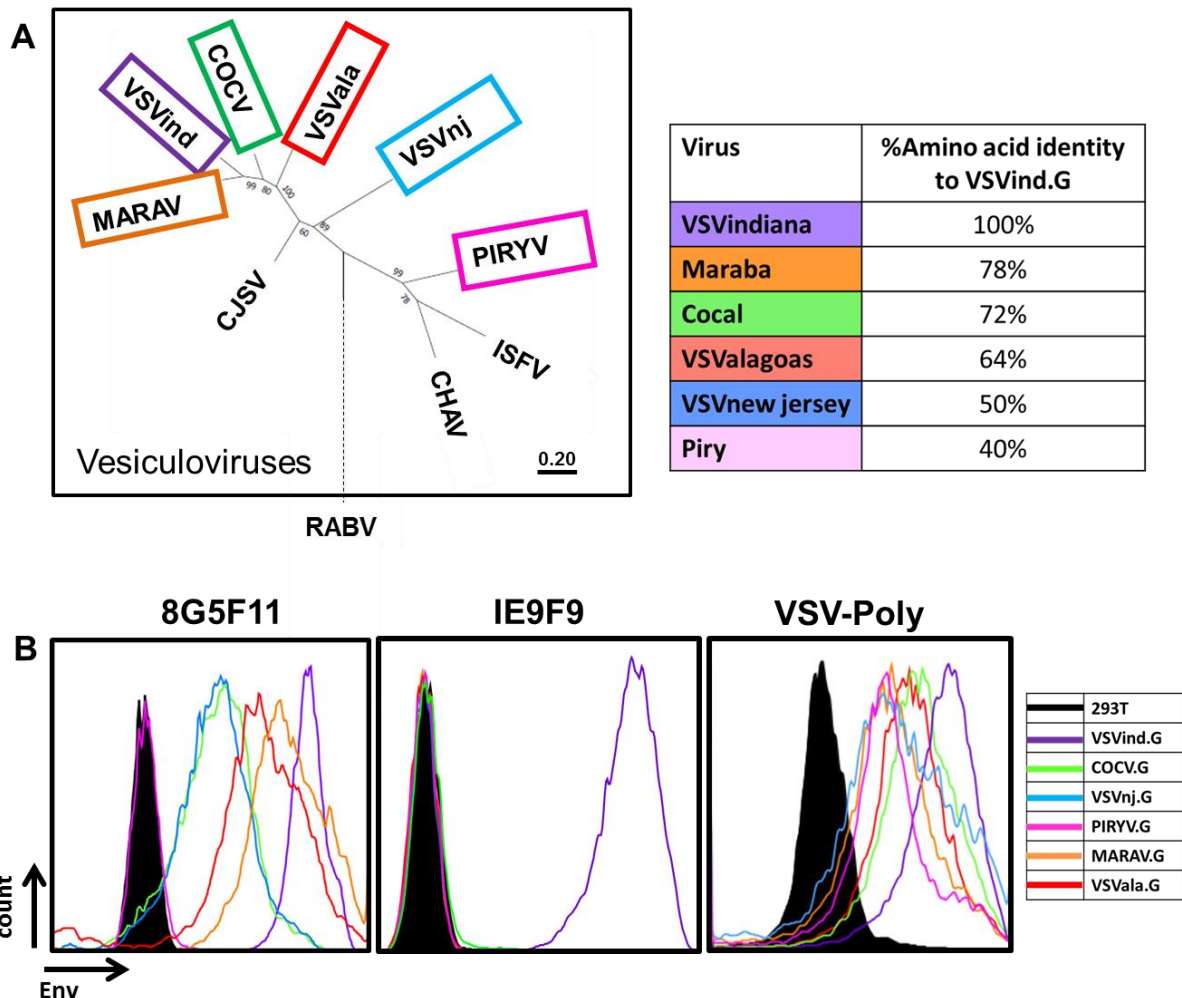
524 bucket rotor (radius 16.1cm). The virus was resuspended in cold plain Opti-MEM on
525 ice, aliquoted and stored at -80°C.

526 **LV titration.** The functional titre of each vector preparation was determined by flow
527 cytometric analysis for GFP expression following transduction of HEK293T cells.
528 Briefly, 2×10^5 /well 293T cells were infected with LV plus 8 µg/ml polybrene (Merck-
529 Millipore, Billerica, MA) for 24 hours. Infected cells were detected by GFP expression
530 at 48 hours following the start of transduction. Titres were calculated from virus
531 dilutions where 1–20% of the cell population was GFP-positive using the following
532 formula:

$$\begin{aligned} 533 \quad & \text{Titre} \left(\frac{\text{transduction units (TU)}}{\text{ml}} \right) \\ 534 \quad & = \frac{(\text{no. of cells at transduction}) \times (\% \text{ of GFP positive cells} \div 100) \times (\text{dilution factor})}{(\text{the volume of virus preparation added (ml)})} \end{aligned}$$

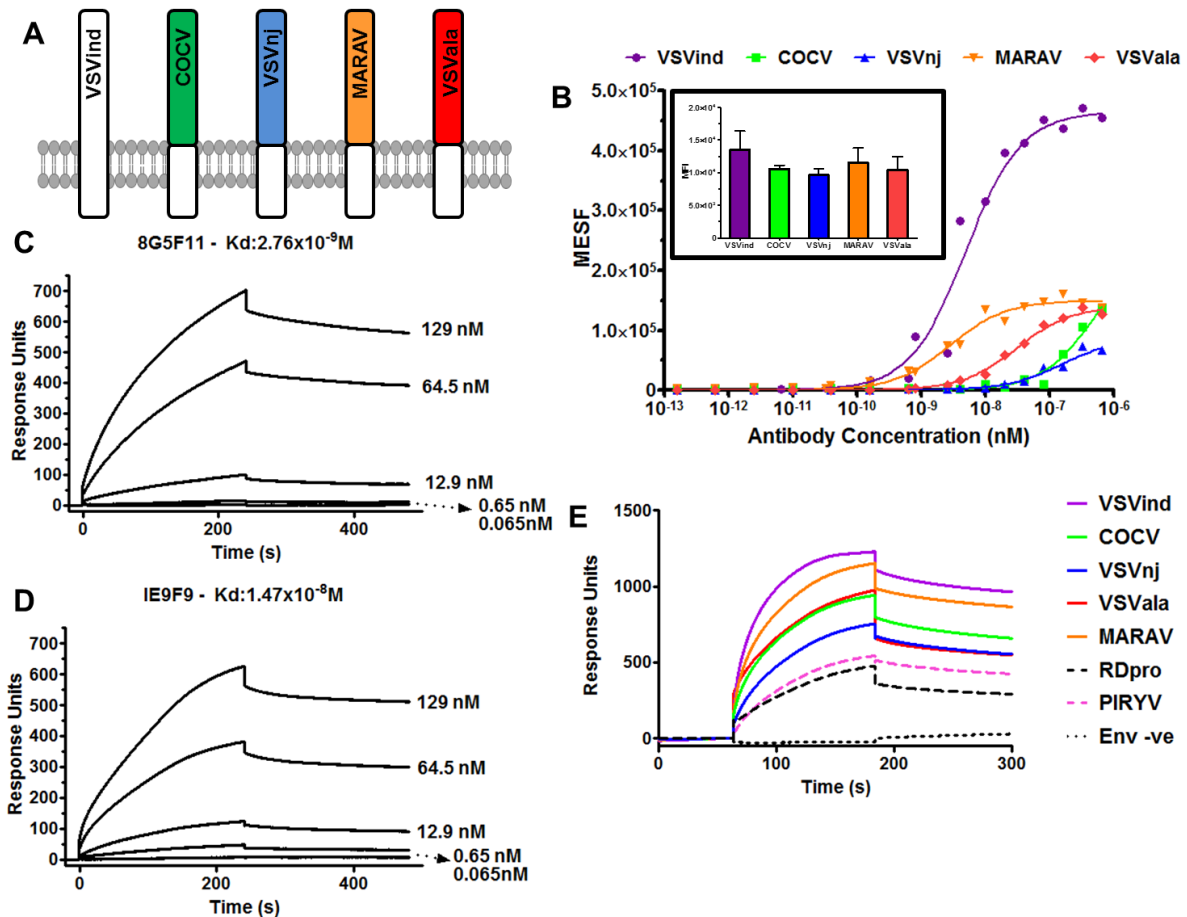
535 **Antibody neutralisation assay.** To determine the neutralisation activity of anti-
536 VSVind.G monoclonal and polyclonal antibodies an infection assay in the presence of
537 antibodies was performed. Briefly, HEK293T cells were seeded in a 96-well plate at a
538 density of 2×10^4 cells/well with 200µl of medium containing 8µg/ml polybrene.
539 Approximately 3 hours later, antibodies were serially diluted in plain Opti-MEM to 12
540 different concentrations/dilutions ranging from 0.5mg/ml (1:2 dilution) to 1.6×10^{-7}
541 mg/ml (1:6,250,000 dilution). Each antibody dilution was mixed 1:1 with VesG-LV or
542 mutant G-LV at 4.0×10^5 TU/ml titre to a final volume of 20µl, incubated at 37°C for 1h
543 and plated on the cells. 48 hours after cells were harvested and analysed for GFP
544 expression by flow cytometry.

545 **Site-directed mutagenesis PCR for production of mutant G proteins for epitope**
546 **mapping.** Site-directed mutagenesis (SMD) method was utilized to produce G protein
547 mutants that were used in epitope mapping experiments. For this, QuikChange II XL
548 Site-Directed Mutagenesis Kit (Agilent, Santa Clara, CA) was used. Initially, primers
549 that would have the desired nucleotide changes were designed using the QuikChange
550 Primer Design Tool (<http://www.genomics.agilent.com/primerDesignProgram.jsp>).
551 All primers used were obtained from Sigma-Aldrich (St Louis, MO). The reaction was
552 carried out according to manufacturer's instructions.



553

554 **Figure 1: 8G5F11 and VSV-Poly cross-react with a variety of VesG while IE9F9**
555 **only binds to VSVind.G.** (A) G proteins of the major vesiculoviruses, as well as the
556 G protein of the rabies virus (RABV), were analysed with regards to their phylogenetic
557 relationship. The tree amongst VesG is drawn to scale, with branch lengths measured
558 in the number of substitutions per site, depicted in the linear scale. VSVind: Vesicular
559 stomatitis virus Indiana strain, COCV: Cocal virus, VSVnj: Vesicular stomatitis virus
560 New Jersey strain, PIRYV: Piry virus, CJSV: Carajas virus, CHAV: Chandipura virus,
561 ISFV: Isfahan virus, MARAV: Maraba virus, VSVala: Vesicular stomatitis virus Alagoas
562 strain. Vesiculoviruses that we investigated are highlighted in boxes and percentage
563 amino acid identities to VSVind.G are summarised in the table on the right-hand side.
564 (B) Histograms represent the binding of the antibodies to the VesG expressed on the
565 surface of transfected HEK293T cells. The strength of cross-reaction is depicted via
566 the different MFIs of the histograms. On the other hand, IE9F9 only bound to
567 VSVind.G. Data shown is one of the three repeats performed.



569

570 **Figure 2: Investigation of 8G5F11 and IE9F9 affinities towards VSVind.G and**

571 **characterisation of 8G5F11 cross-reactivity. (A)** Schematic representation of the

572 chimeric vesiculovirus G proteins with VSVind.G transmembrane and C-terminal

573 domains. **(B)** HEK293T cells expressing chimeric VesG were incubated with serial

574 dilutions of 8G5F11 and analysed via flow cytometry. MFIs of the fluorescent signals

575 were converted into the number of fluorophores using the MESF standard curve

576 according to manufacturer's instructions, the background signal from mock-

577 transfected HEK293Ts was subtracted and binding saturation curves were plotted.

578 The varying affinity of the mAb towards different VesG is demonstrated by the shift in

579 the slope of the binding curves. The curves were fitted, and dissociation constants

580 (Kd) calculated using the software GraphPad Prism 5 modelling the interaction as 1:1

581 specific binding: VSVind.G: $2.64 \times 10^{-9} M$, COCV.G: $5.88 \times 10^{-7} M$, VSVnj.G: $1.57 \times 10^{-7} M$,

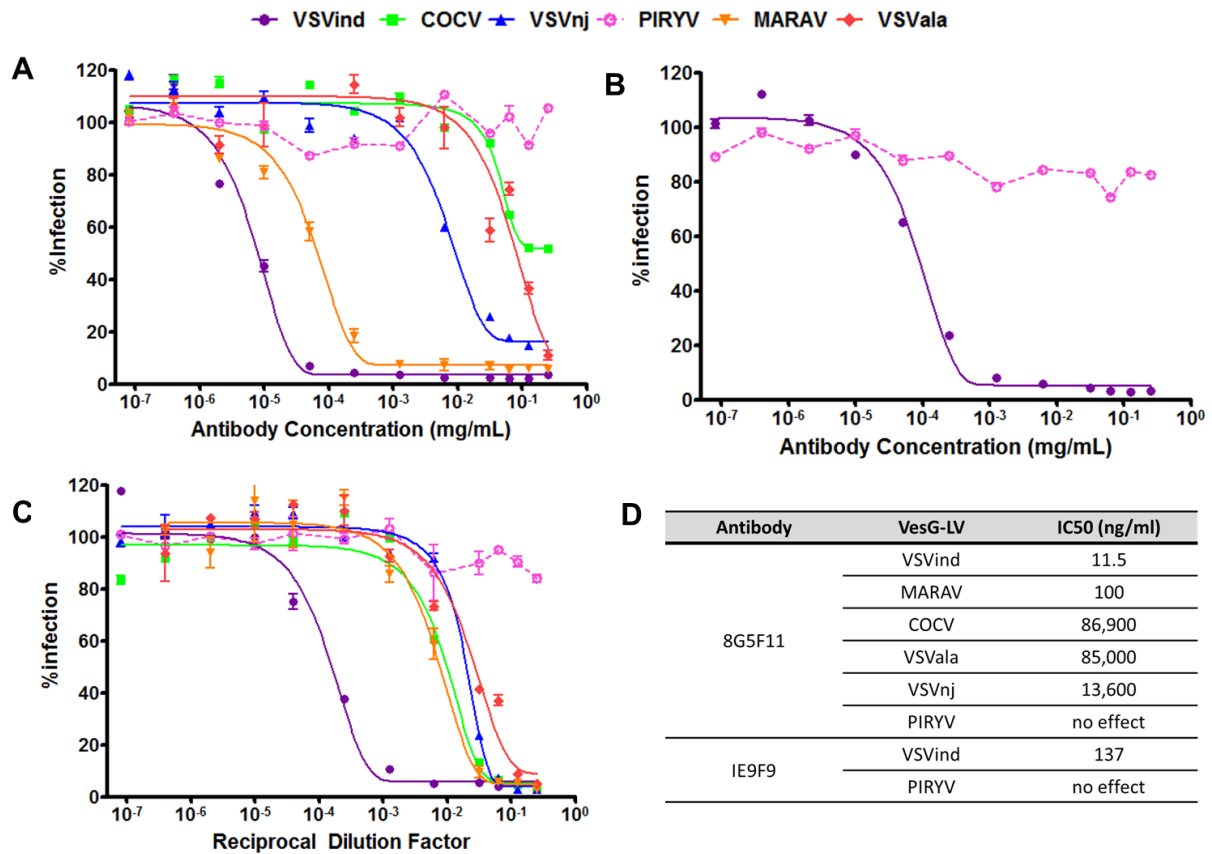
582 MARAV.G: $4.13 \times 10^{-9} M$, VSVala.G: $3.09 \times 10^{-9} M$. Data shown represent the mean of

583 three repeats performed in duplicates. **(inset)** The expression levels of the chimeric G

584 proteins were determined via intracellular P5D4 staining. Data shown represent the

585 mean +/- SD of three repeats performed in duplicates. Surface plasmon resonance
586 (SPR) analysis of **(C)** 8G5F11 and **(D)** IE9F9 binding to immobilized Gth in HBS-EP
587 buffer. **(E)** Surface plasmon resonance analysis of Ves.G-LV (1×10^8 TU/ml) binding
588 to immobilized 8G5F11 in HBS-EP buffer. The binding curves are normalised with
589 regards to the relative response of unenveloped LV particles (Env -ve) which is
590 regarded as the background. SPR data shown is one of the three repeats performed.

591

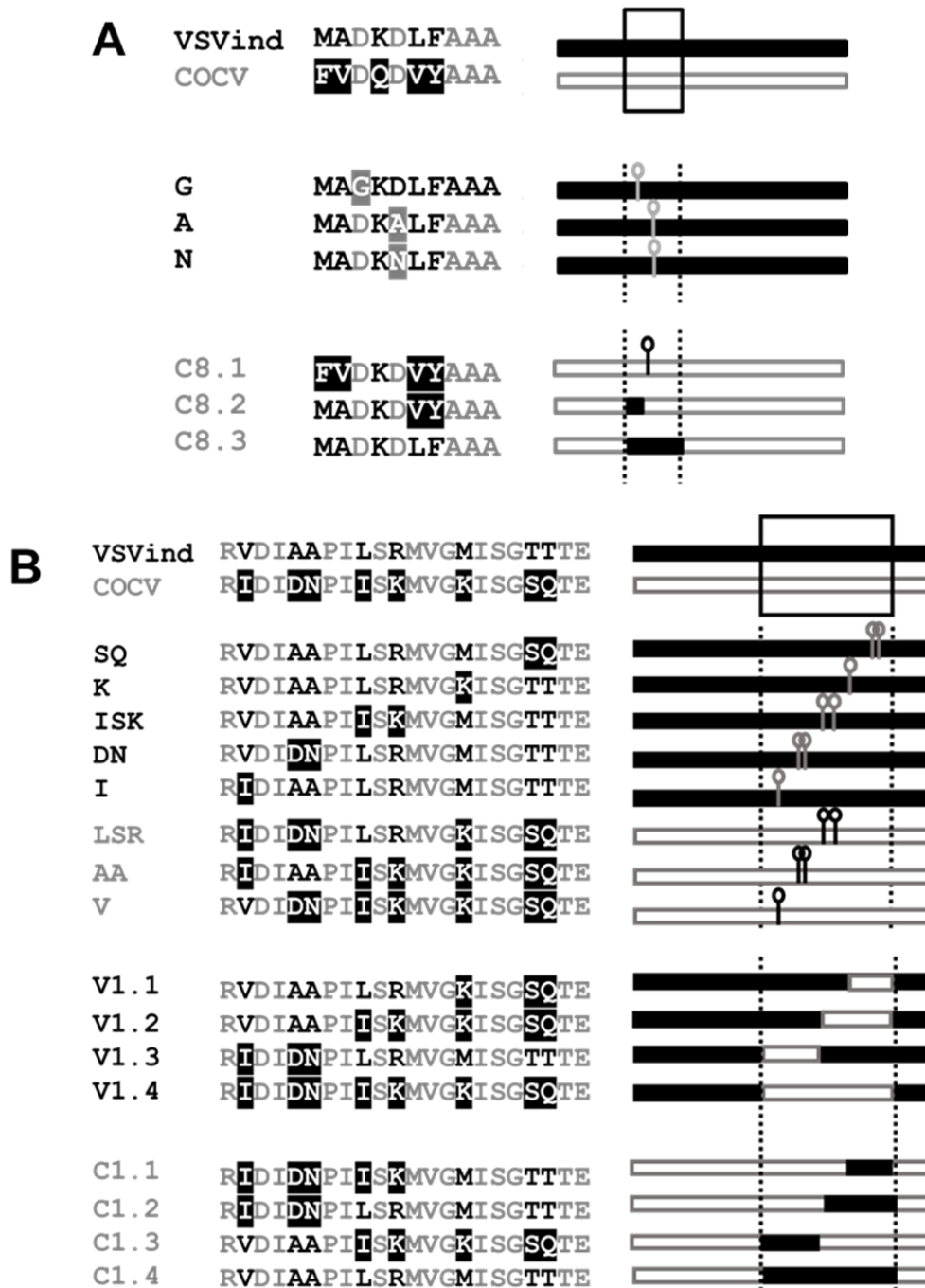


592

593 **Figure 3: Neutralisation activity of mAbs and VSV-Poly.** Neutralisation of VesG-
 594 LV by (A) 8G5F11, (B) IE9F9, and (C) VSV-Poly. Solid lines signify the neutralisation
 595 effect observed while the dotted lines indicate the lack of neutralisation. (D) Calculated
 596 IC50 values for 8G5F11 and IE9F9, depicting the potency of neutralisation. The
 597 curves were fitted using the software GraphPad Prism 5 modelled as an [inhibitor] vs.
 598 response curve with variable Hill Slopes and IC50 values calculated. Data shown
 599 represent the mean +/- SD of three repeats.

600

601

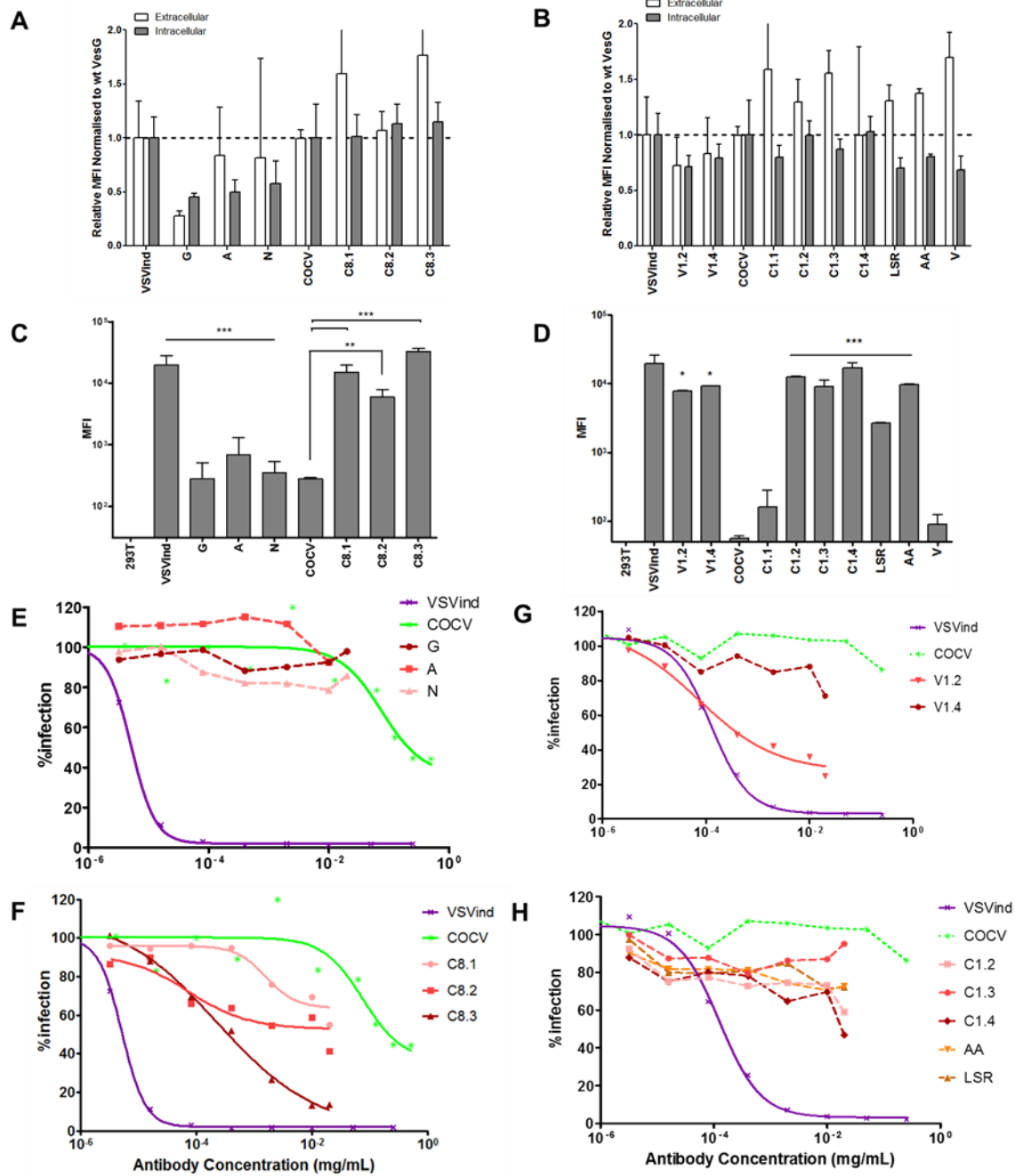


602 **Figure 4: Mutants and chimeric G proteins produced for epitope mapping.**

603 Mutants and chimeras produced for epitope mapping of monoclonal antibodies (A)
 604 8G5F11 and (B) IE9F9. Names and linear representations of the mutants and
 605 chimeras are listed on either side of the amino acid alignments of the regions where
 606 mutations were made. Amino acid alignment legend: Black; residues from wt
 607 VSVind.G, white with black background; residues from wt COCV.G, grey; shared
 608 residues, white with grey background; previously identified mutants (15). Linear G
 609 protein representations: the regions that the mutations were carried out at are

610 represented by dotted lines. Black bars represent wt VSVind.G sequences while grey-
611 bordered bars are for wt COCV.G residues. Point mutations are denoted by a bar and
612 a circle.

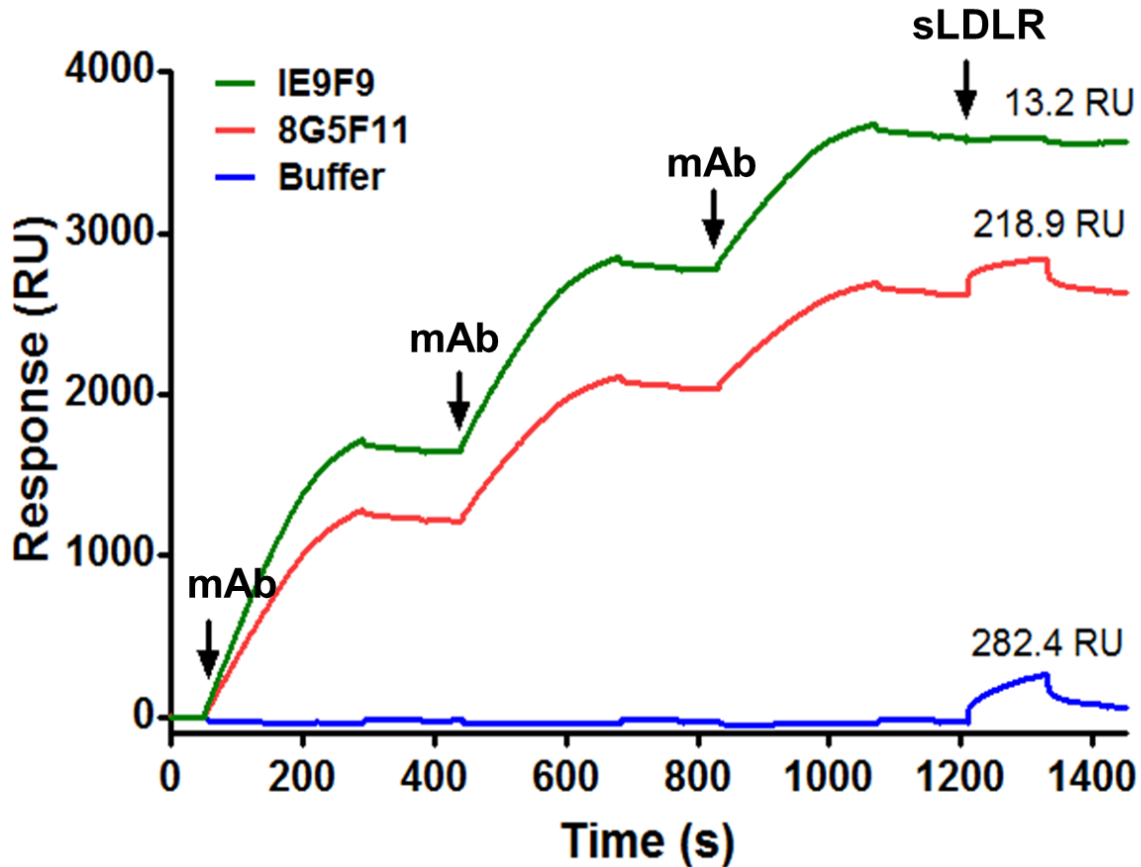
613



614 **Figure 5: Investigation of antibody binding to mutant G proteins and**
 615 **neutralisation of mutant-LVs.** HEK293T cells were transfected to express the mutant
 616 G proteins on their surface. (A-B) The cells expressing chimeric mutants were stained
 617 with extracellular VSV-Poly (white bars) and intracellular P5D4 (grey bars) as
 618 expression control for the G proteins. The measured MFI values were normalised to
 619 the wt VesG signals for each set of mutants. The same population of cells were also
 620 incubated with (C) 8G5F11 and (D) IE9F9 at saturating concentrations. One-way
 621 ANOVA analysis with Dunnett's post-test was performed to compare the MFI values
 622 of mutant G proteins to that of their wild-type counterpart. Legged lines denote the

623 significance of a single comparison, while straight lines signify all the individual
624 comparisons within the group share the denoted significance unless otherwise stated
625 (*, $p < 0.05$; **, $p < 0.01$; ***, $p < 0.001$). This assay was performed three times in
626 duplicates; mean \pm SD is plotted above. The neutralisation curves for select mutant
627 and chimeric G pseudotyped LVs are plotted for **(E-F)** 8G5F11 and **(G-H)** IE9F9. Solid
628 lines signify the neutralisation effect observed. **(E-G)** Previously reported reductions
629 in binding for VSVind.G mutants translated into either complete or partial resistance
630 to neutralisation by both antibodies. For COCV.G mutants **(F-H)**, the mutations
631 conferred the G proteins sensitivity to neutralisation by 8G5F11 but not by IE9F9. The
632 curves were fitted using the software GraphPad Prism 5 modelled as an [inhibitor] vs.
633 response curve with variable Hill Slopes. Data shown represent the mean from three
634 experiments performed in independent triplicates.

635



636 **Figure 6: IE9F9 hinders sLDLR binding to Gth.** 8G5F11 and IE9F9 were injected
637 over immobilised Gth at 10 μ g/ml concentration three times to achieve binding
638 saturation. Following this, sLDLR was injected over the chip at a concentration of
639 10 μ g/ml and its binding to Gth was measured. As buffer control an identical sLDLR
640 injection was performed following multiple injections of HBS-EP running buffer.
641 Measured sLDLR binding levels are indicated above the binding response curves
642 and times of injections are marked with arrows. The data presented represent one
643 of the three repeats performed.

644

645 **Funding**

646 AMM and MT studentships are funded by NIBSC.

647 **Acknowledgements**

648 We would like to thank Dr Hiroo Hoshino and Dr Atsushi Oue (Gunma University,
649 Japan), for providing us with a sample of the polyclonal goat anti-VSVind.G antibody,
650 VSV-Poly and Drs Yves Gaudin and Aurélie Albertini for the Gth protein.

651 **Author Contributions**

652 AMM performed experiments to obtain presented data and wrote the paper. MT
653 designed and produced the initial COCV.G/VSVind.G chimeras and obtained
654 preliminary data on 8G5F11 binding to COCV.G bearing cells. GM and MH helped
655 designing experiments and interpreting data. MKC and YT supervised the study and
656 wrote the paper.

657 **Additional Information**

658 **Supplementary information** – accompanies this manuscript.

659 **Competing financial interest** – Authors declare no competing financial interests.